SCIENTIFIC AND TECHNICAL SECTION

UDC 539.4

Modal Analysis of the Turbine Blade at Complex Thermomechanical Loads

L. Witek[1] and F. Stachowicz

Rzeszów University of Technology, Faculty of Mechanical Engineering and Aeronautics, Rzeszów, Poland

[1] lwitek@prz.edu.pl

The results of modal analysis of the turbine blade were presented. The turbine blade during the operation of the engine is subjected to complex thermomechanical loads induced by centrifugal forces of the rotating blade and a nonuniform thermal field. These loads have a great influence on the natural frequencies of the blade. In the first section of the study, modal analysis of the blade was performed using the vibration system. As a result, the resonant frequencies of the real blade were obtained. In order to check the effect of the rotational engine speed and the thermal field on the natural frequencies of the blade, the finite element method was employed. At the first stage of computations static analysis was conducted for the blade subjected to mechanical and thermal loads. Then modal analysis was used to isolate the natural frequencies and vibration modes of the blade. In modal analysis the stress state from the first stage was considered as preliminary conditions. Several results of numerical calculations and experimental analysis were compared to detect the relative error of natural frequency estimates.

Keywords: turbine blade, stress analysis, finite element method, vibration, modal analysis.

Introduction. The turbine blades have small bending stiffness and are particularly susceptible to resonant vibrations. In operation of the engine, the blades are excited by an unbalanced rotor. In the worst case, the excitation frequency overlaps the resonant frequency of the blade. During the resonance, a high stress amplitude results in high-cycle fatigue, thus the blade can be damaged after relatively short time. If a problem arises in the turbine section, it will significantly affect the whole engine function and safety of the aircraft. Failures of any high-speed rotating components can be dangerous to passengers and personnel.

The problem of turbine failure was the subject of several investigations [1–4]. The results of stress, fracture and modal analysis of the turbine and compressor blades were described in [5–11]. The results [12] show that the vibrations have a negative influence on the fatigue life of the aircraft engine blades. The fatigue process of aircraft components can be also accelerated with corrosion [13, 14]. The investigations of vibration analysis of the blades are described in [15–18].

The main objective of this study is to determine the resonant frequencies and free vibration modes of the turbine blade subjected to complex thermomechanical loads. The effect of the rotational turbine speed on the natural frequencies of the aircraft engine blade was additionally analyzed.

1. **Experimental Modal Analysis of the Blade**. Experimental modal analysis of the blade made use of an Unholtz-Dickie UDCO TA-250 vibration system presented in Fig. 1a. The blade was horizontally mounted on the movable head of the vibrator (Fig. 1b). In

modal analysis the excitation frequency was increased from 500 to 4000 Hz with the sweep rate of 1 Hz/s. The intensity of excitation was defined as $2g$ (where $g = 9.81$ m/s^2).

In experimental analysis two measurement channels were activated. The first channel was used to measure the acceleration amplitude of the vibrator head (signal A_1). The acceleration in this channel was measured by a large sensor (10g). The signal (A_2) in the second channel was delivered from the miniature piezoelectric acceleration sensor (0.2g) (Fig. 1b). This sensor was located 15 mm above the bottom of the blade airfoil section. This position is more advantageous than the location of the sensor on the top of the blade. The sensor position closer to the blade fir-tree slot (blade constraint) causes smaller disturbances in dynamics of an investigated object. The acceleration sensors were connected to the blade with special wax.

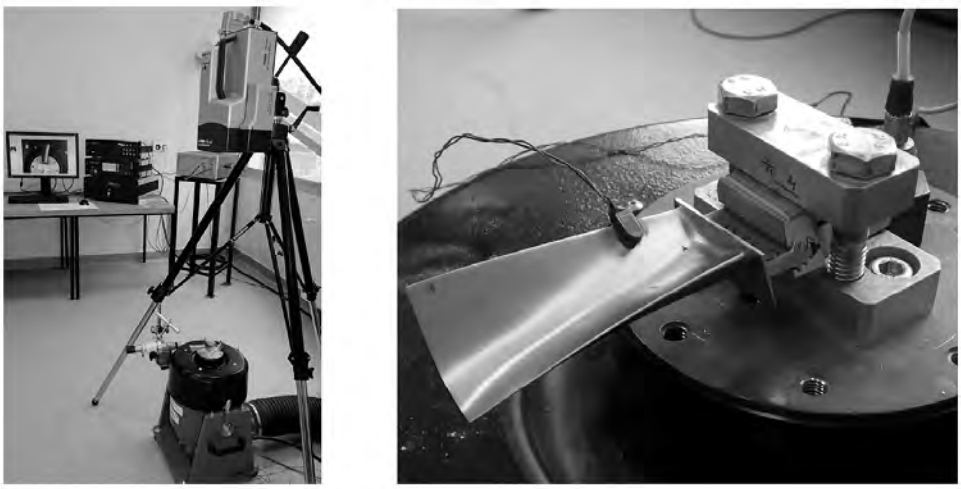

a b

Fig. 1. Vibration system for experimental modal analysis (a) and the blade fixed to the head of the vibrator (b).

During modal analysis the excitation frequency was gradually increased. At this time the signals from the two measurement channels were recorded. The main result of modal analysis is the amplitude-frequency characteristic shown in Fig. 2. On the horizontal axis the actual excitation frequency is plotted. The relative amplitude of the blade is laid off on the vertical axis. The relative amplitude is the ratio of the acceleration amplitude from the second channel (A_2) to the signal from the first channel (acceleration amplitude of the vibrator head, A_1).

As is seen in Fig. 2, a high peak typical of a resonance phenomenon is observed at 969.7 Hz. This value is the resonant frequency (vibration mode I). The relative amplitude of vibration I mode equals 119.11. The second peak is visible on the amplitude-frequency characteristic at 2585.2 Hz. This value is the resonant frequency for vibration mode II. The third resonant frequency equals 3727.4 Hz (Fig. 2).

2. **Numerical Model of the Blade, Loads and Boundary Conditions**. The numerical model of the turbine blade was constructed using an MSC-PATRAN program [19]. The model reproduces the geometry of the real blade (Fig. 3a). The discrete model of the turbine blade presented in Fig. 3b consists of 353478 TET-4 finite elements (with linear function [20]) and 70754 nodes. The average size of elements equals 0.54 mm. The material of the blade (EI-437-y nickel alloy) was defined as linear elastic with the following properties: modulus of elasticity = 200 GPa, Poisson's ratio = 0.3, and density = 8200 kg/m^3 [21]. An

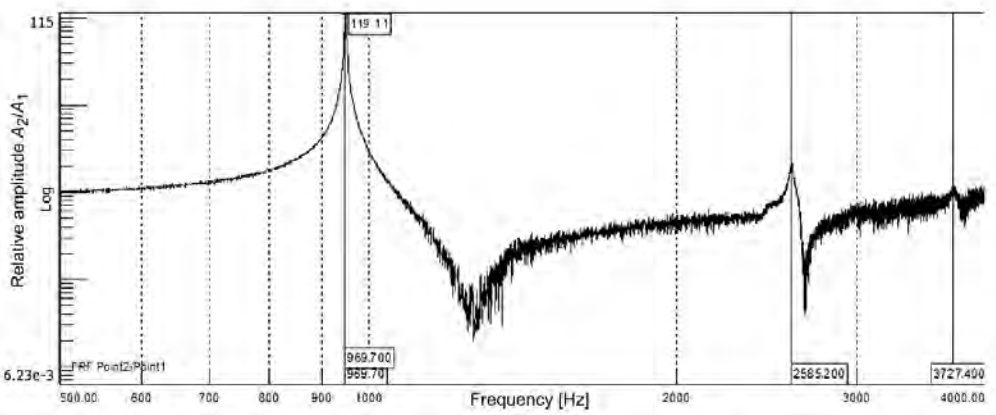

Fig. 2. Amplitude–frequency characteristic for an examined turbine blade.

a b c

Fig. 3. Object of investigations (a), numerical model of the blade (b), and the temperature field in the blade during the operation of the engine [height $h = 2500$ m and engine power of 900 HP (662 kW)] (c).

EI-437-y alloy has a good creep resistance and was used for hot rotational components of turbine engines.

In modal analysis the surfaces of the fir-tree slots (blade lock) were totally constrained ($T_x = T_y = T_z = 0$). The thermal field on the turbine (considered in Sect. 4) was shown in Fig. 3c. The modulus of elasticity and the thermal expansion coefficient for an EI-437-y alloy were assumed to be temperature-dependent.

3. **Results of Numerical Modal Analysis**. Numerical modal analysis was performed using an ABAQUS solver [20]. As a result of computations, the modes and natural frequencies of the blade were obtained. At the first stage of the analysis, the rotational speed of the engine rotor was defined as $n = 0$ whereas the constant temperature was equal to $T = 0$°C (only the blade was fixed). These conditions were employed in experimental modal analysis of the blade.

The results of computations demonstrated that the resonant frequency (for vibration mode I) equalled 992 Hz (Table 1). The experimental result is equal to 969.7 Hz.

To estimate the validity of the numerical solution, the relative error E was defined by the formula:

$$E = \frac{F_{res} - F_{nf}}{F_{res}} \cdot 100\%, \tag{1}$$

where F_{res} is the resonant frequency (experimental result) and F_{nf} is the natural frequency (numerical result).

The relative error E (mode I) equals 2.3% (Table 1). For vibration mode II the error is 3%. A greater relative error (10.2%) is observed for free vibration mode III. The results from the next modes cannot be compared because of limitations of a UDCO TA-250 vibration system used in experimental investigations (5–4000 Hz).

Table 1

Comparison of Experimental and Numerical Results ($n = 0$, cold blade $T = 0$°C)

Natural frequency/resonant frequency								
Mode I			Mode II			Mode III		
F_{nf}, Hz	F_{res}, Hz	E, %	F_{nf}, Hz	F_{res}, Hz	E, %	F_{nf}, Hz	F_{res}, Hz	E, %
992	969.7	2.3	2663	2585.2	3.0	4108	3727.4	10.2

4. **Effect of the Thermal Field and Rotational Turbine Speed on the Natural Frequency of the Blade**. The rotation of the engine rotor induces large centrifugal stresses in the blade. Tensile stresses cause an increase in the natural frequencies of the blade during the acceleration of the turbine. High temperatures on the turbine blade also exert influence on its natural frequency. This complex phenomenon is associated with a decrease in the modulus of elasticity of the blade material at high temperatures. Additionally, the hot blade has a larger size (because of thermal expansion), which influences a decrease in the natural frequencies as well. In this section the effect of the rotational turbine speed and thermal field on the natural frequencies of the blade was investigated.

For solving the problem, the procedure of numerical analysis was divided into the three stages. At the first stage of static analysis, the thermomechanical loads were applied to the blade. As a result, the stress distribution for the blade subjected to rotational speeds and nonuniform thermal fields was obtained. At the second slage modal analysis of the blade was performed using an ABAQUS command: *Frequency* [20]. At the third stage *Complex frequency* analysis [20] was used to isolate the natural frequencies of the blade. In this procedure, the stress state reached at the first stage (for the hot blade subjected to rotation) is considered a preliminary condition for modal analysis.

The equivalent stress distributions (according to the Huber–Mises–Hencky criterion) for free vibration modes I, II, and III of the blade are presented in Fig. 4. The results correspond to the maximum vibration amplitude of the blade $A = 1$ mm. The maximum stress area for mode I (296 MPa, Fig. 4a) is located in the zone above the blade lock. Mode I can be classified as pure flexural (Table 2).

For free vibration mode II the maximum stress area (229 MPa) is located in the blade airfoil section. Mode II can be classified as torsional-flexural (combination of torsion and bending).

Free vibration mode III is pure torsional. The large stress area in this case is located on the leading edge of the blade (743 MPa). Maximum stresses obtained in modal analysis

T a b l e 2

Classification of Free Vibration Modes of the Blade

Mode number	I	II	III	IV	V	VI
Mode shape (classification)	flexural	torsional-flexural	torsional	complex	complex	complex

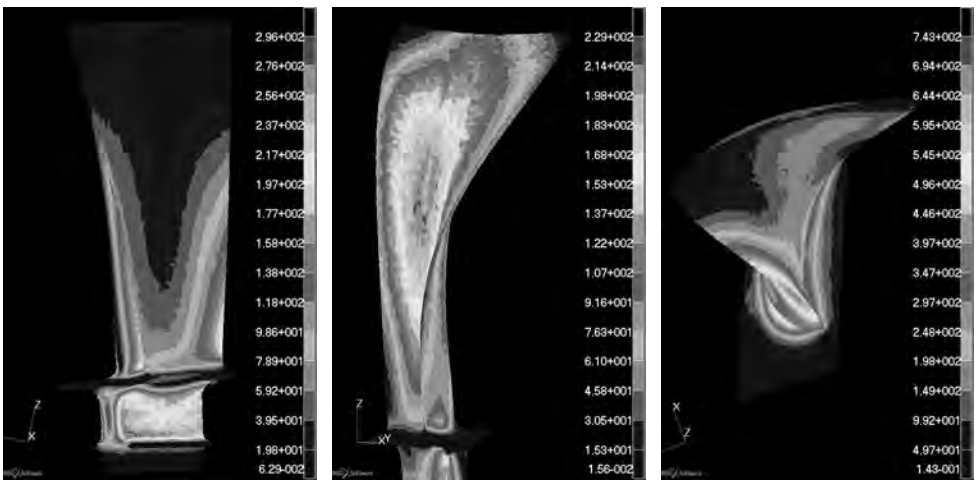

a b c

Fig. 4. Equivalent stress distributions (according to the Huber–Mises–Hencky criterion) in the turbine blade for free vibration modes I (a), II (b), and III (c) (blade amplitude $A = 1$ mm, $n = 22{,}490$ rpm, thermal field).

should be treated as reliable results. The stress at the blade resonance depends on the real vibration amplitude of the blade.

The results of modal analysis for the blade subjected to rotational speeds and thermal fields (Fig. 3c) are summarized in Table 3. The maximum rotational speed of the engine rotor (22,490 rpm) should be related to a 100% speed of the turbine. In this study the following speeds: 0, 50, 80, and 90% were used. Moreover, the overspeed condition of the turbine (110%) was also considered.

The results of the two analyses are depicted in Fig. 5. Curve *1* is related to the rotating blade in the nonuniform thermal field (Fig. 3c). Curve *2* presents the natural frequencies of the cold rotating blade (without specifying the temperature).

As is seen in Fig. 5, the natural frequency of the cold blade for the rotor speed of 0% equals 992 Hz (Table 1). After acceleration of the turbine to the speed of 100%, the natural frequency of the cold blade is equal to 1178 Hz (increase by about 19%).

After heating the blade to the operation temperature (Fig. 3c), the natural frequency (for the rotor speed of 0%, mode I) equals 908 Hz (Fig. 5, Table 3). It means that the thermal field (for $n = 0$) causes a decrease in the natural frequency by about 8.4%. After acceleration of the hot blade to the speed of 100%, the natural frequency increases to 1112 Hz (increase by about 21%).

For free vibration mode II the natural frequency of the hot blade increases from 2419 Hz to 2586 Hz (increase by 7%) (Fig. 6, Table 3).

In the torsional vibration mode (mode III) the natural frequency of the blade (increase in frequency by about 1.7%) is slightly influenced by the rotational speed of the turbine (Fig. 6, Table 3). In this case the tensile stress of the rotating blade exerts little influence on the shear stress arising during the torsional vibration of the blade.

T a b l e 3

Natural Frequencies of the Blade for Different Rotational Speeds of the Turbine [Thermal Fields of the Blade for the Engine Operation at $h = 2500$ m, Engine Power of 900 HP (662 kW)]

Turbine speed [%]	Turbine speed [rpm]	Natural frequency [Hz]					
		Mode I	Mode II	Mode III	Mode IV	Mode V	Mode VI
0	0	908	2419	3741	4855	6031	9366
50	11,245	954	2456	3758	4893	6083	9398
80	17,992	1021	2511	3776	4951	6165	9446
90	20,241	1050	2534	3785	4977	6202	9466
100	22,490	1079	2559	3798	5005	6239	9487
110	24,739	1112	2586	3804	5036	6281	9509

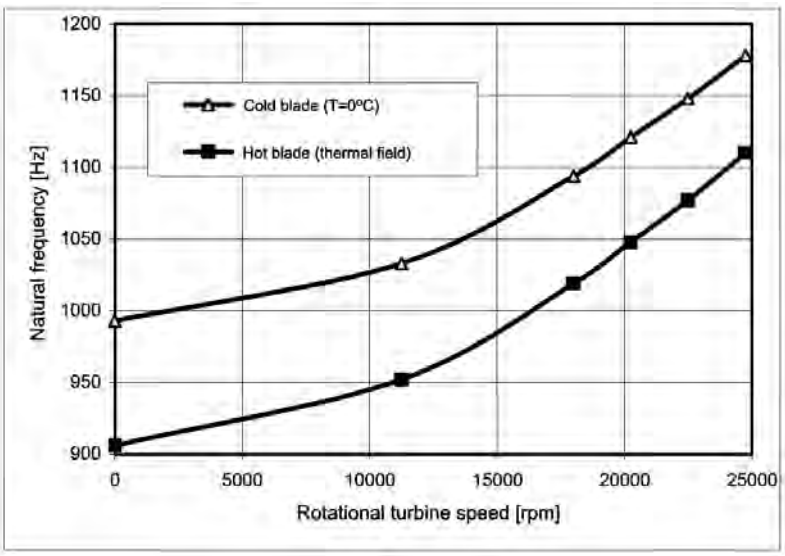

Fig. 5. Effect of the rotational turbine speed on the natural frequencies of the cold and hot blades (vibration mode I).

Conclusions. In this study the effect of the rotational speed of the engine rotor and the thermal field in the turbine on the natural frequencies of the blade was investigated. In the first section of the study experimental analysis was performed to determine the real resonant frequencies of the turbine blade. In the next section numerical modal analysis of the blade (with consideration of the rotational turbine speed and the nonuniform thermal field on the blade) was conducted. As a result, the free vibration modes and frequencies of the cold and hot rotating blades were determined.

This study give rise to the following findings.

1. The relative error of the numerical solution (natural frequency estimates) makes up 2.3% (mode I), 3.0% (mode II), and 10.2% (mode III).

2. A considerable error (10.2%) for vibration mode III can be caused by large-sized finite elements of the numerical model of the blade. Convergence of numerical solutions obtained with different types and number of finite elements in the model (with parabolic function) was corroborated.

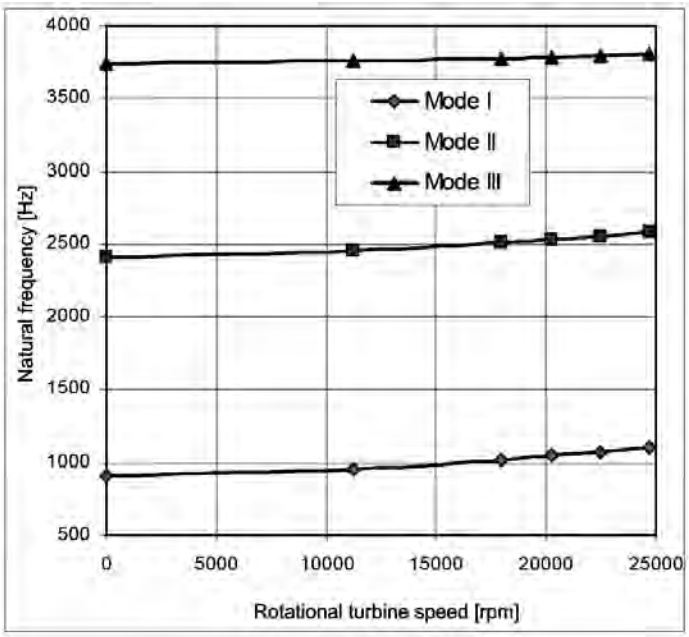

Fig. 6. Effect of the rotational turbine speed on the natural frequencies of the hot blade (free vibration modes I, II, and III).

3. The operation temperature on the turbine causes a decrease in the natural frequency of the blade by about 8%.

4. The natural frequencies of the hot blade for modes I and II (after turbine acceleration from $n = 0$ to 22,490 rpm) increase by 21% and 7%, respectively.

5. The natural frequency (for mode III) of the rotating blade increases only by 1.7%. The centrifugal forces of the rotating blade exert little influence on the shear stress arising during pure torsional vibration.

Acknowledgments. The research received funding from the People Programme (Marie Curie International Research Staff Exchange) of the European Union's Seventh Framework Programme FP7/2007-2013/ under REA Grant PIRSES-GA-2013-610547.

1. W. Maktouf and K. Sai, "An investigation of premature fatigue failures of gas turbine blade," *Eng. Fail. Anal.*, **47**, 89–101 (2015).
2. M. Park, Y. H. Hwang, Y. S. Choi, and T. G. Kim, "Analysis of a J69-T-25 engine turbine blade fracture," *Eng. Fail. Anal.*, **9**, 593–601 (2002).
3. K. S. Song, S. G Kim, D. Jung, and Y. H. Hwang, "Analysis of the fracture of a turbine blade on a turbojet engine," *Eng. Fail. Anal.*, **14**, 877–883 (2007).
4. L. Witek, "Failure analysis of turbine disc of an aero engine," *Eng. Fail. Anal.*, **13**, 9–17 (2006).
5. S. K. Chan and I. S Tuba, "A finite element method for contact problems of solid bodies – Part II: Applications to turbine blade fastenings," *Int. J. Mech. Sci.*, **13**, 627–639 (1971).
6. L. Witek, "Fatigue investigations of the compressor blades with mechanical defects," *Key Eng. Mater.*, **598**, 269–274 (2014).
7. L. Witek, "Simulation of crack growth in the compressor blade subjected to resonant vibration using hybrid method," *Eng. Fail. Anal.*, **49**, 57–66 (2015).

8. Akash Shukla and S. P. Harsha, "An experimental and FEM modal analysis of cracked and normal steam turbine blade," *Materials Today: Proceedings*, **2**, 2056–2063 (2015).
9. P. Papanikos, S. A. Meguid, and Z. Stjepanovic, "Three-dimensional nonlinear finite element analysis of dovetail joints in aeroengine discs," *Finite Elem. Anal. Design*, **29**, 173–186 (1998).
10. T. Gwo-Chung, "Rotating vibration behavior of the turbine blades with different groups of blades," *J. Sound Vibr.*, **271**, 547–575 (2004).
11. E. Poursaeidi and B. Hosein, "Fatigue crack growth simulation in a first stage of compressor blade," *Eng. Fail. Anal.*, **45**, 314–325 (2014).
12. L. Witek, "Crack growth simulation in the compressor blade subjected to vibration using boundary element method," *Key Eng. Mater.*, **598**, 261–268 (2014).
13. A. Poznanska, M. Sniezek, and M. Wierzbinska, "Pitting corrosion – main factor generating fracture of the compressor of aeroengine blades under operation," in: Proc. of IX Conference – Turbomachinery [in Polish], Rzeszow (2003).
14. L. Witek, "Failure analysis of the wing-fuselage connector of an agricultural aircraft," *Eng. Fail. Anal.*, **13**, 572–581 (2006).
15. S. I. Bogomolov, S. S. Lutsenko, and S. A. Nazarenko, "Application of a superparametric finite shell element to the calculation of turbine blade vibrations," *Strength Mater.*, **14**, No. 6, 796–799 (1982).
16. X. S. Yao and C. L. Zheng, "Shaking-swing coupled vibration analysis of a laminar composite rotating blade by the finite element method," *Strength Mater.*, **47**, No. 1, 68–73 (2015).
17. V. T. Troshchenko, V. S. Kostenko, A. P. Voloshchenko, et al., "Automatic system of programmed control of parameters of vibration and thermal tests of gas turbine engine blades (ASPC VTT)," *Strength Mater.*, **22**, No. 1, 128–132 (1990).
18. R. P. Pridorozhnyi, A. V. Sheremet'ev, and A. P. Zinkovskii, "On the rational choice of the azimuthal crystallographic orientation of single-crystal cooled rotor blades in aircraft gas turbine engines," *Strength Mater.*, **47**, No. 3, 415–421 (2015).
19. *MSC-PATRAN 2009 Users Manual*, MSC Corporation, Los Angeles (2009).
20. *ABAQUS ver. 6.9 Users Manual*, Abaqus Inc. (2009).
21. P. B. Mikhailov-Mikheev, *Handbook on Metallic Materials for the Construction of Turbines and Engines* [in Russian], Mashgiz, Leningrad (1961).

Received 10. 08. 2016